# Construction of Low-pass HV Filter for Measuring of Partial Discharge

Bohumil Skala, Vaclav Kus, Vladimir Kindl
Dept. of Electromechanic and Power electronic
University of West Bohemia
Pilsen, Czech republic
skalab@kev.zcu.cz

Petr Mraz
Haefely Test AG
Basel, Switzerland
mraz.petr@haefely.com

***Abstract*—The paper discusses methodology for construction of low-pass high voltage (HV) filter for measuring of partial discharge deteriorating the insulating system of electric machinery. It focuses mainly on the shape optimization using analytical approach with subsequent verification using finite element method. It also gives an overview of filter characteristics for its different shape.**

***Keywords—low-pass filter; partial discharge; magnetic field; finite element method***

## I. INTRODUCTION

Every complex electrical device is inherently and unavoidably dangerous to fail in operation due to many external/internal matters (e.g. excessive electrical, thermal or mechanical stress, extreme operating conditions …) [1-4]. A proper diagnostic system may signalize and consequently forestall such oncoming failure causing enormous financial losses and problems related with forced outage of the device. One of the most followed parameter for electric machinery is partial discharge (PD) activity in insulating system having negative impact on its life-time. The literature usually divides PD in two groups. The first, slot discharges are discussed at global scale from the early 1950s up to the present day literature [5, 6]. The second, surface discharges take place mainly in the overhang part of the stator winding with rated voltage higher than 3 kV. This sort of PD can be significantly reduced by application of semi-conductive paints or tapes [7-10].

Detection and evaluation of PD activity [11-15] is therefore very important issue for systems reliability. Precise determination of actual condition of the insulating system may prevent its destructive changes and plan lay-offs or regular maintenance. Nowadays, the PD detection as a non-destructive diagnostic tool is used in a wide range of applications, e.g. in case of generators, transformers, cables, switchgears and many others. One of the most common test circuit of galvanic PD measurement method (according to IEC 60270) can be seen in Fig. 1.

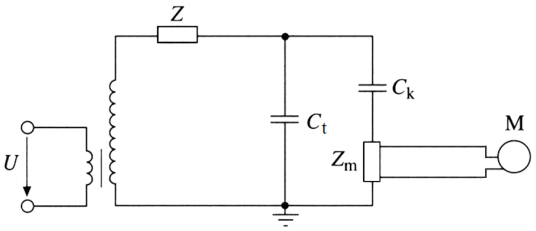


Figure 1. Basic PD measurement test circuit [13].

The measuring circuit is supplied from high voltage power source $U$ with sufficiently low level of internal noise. The filter $Z$ must be connected on the output of the source to block any disturbance and to prevent potential leakage of PD current pulses going through. While the filter is mostly build as a large inductance the tested insulating systems $C_t$ exhibits predominantly capacitive character. The coupling capacitor $C_k$ covers the voltage drop caused by the PD events. This voltage drop is scanned by the measuring impedance $Z_m$ and transferred using measuring device $M$ to the current impulse (or in other words the charge).

The HV filter plays very important role in case of diagnosis of rotating machines and transformers where the HV cable is used to energize the DUT (device under test). The measured PD signal may contain due to the long power cable additional oscillations, reflections and attenuation and must be therefore filtered (see Fig. 2).

The filtering air-cored coil can be considered as a RLC network with complex mutual interconnection. While the coils inductance influences mainly the resonance frequency of the filter, the capacitance

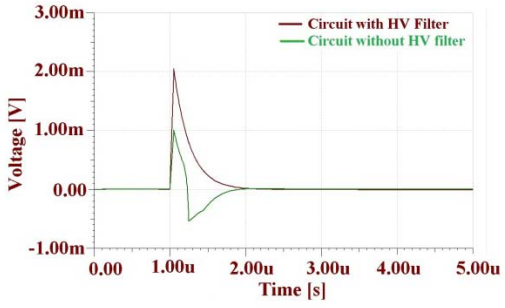


Figure 2. Influence of HV power cable to the HF PD signal.

ISBN 978-80-261-0386-8, 

affects its attenuation. Hence it is desire to maximize the inductance to get the high pass frequency as low as possible (close to the 80 kHz – 140 kHz). Consequently the capacitance should be very low to reach as highest attenuation as possible.

## II. Filter Design and FEA Verification

The modern design method of new industrial device usually includes many technical requirements and electrical and space limitations. In the past, the process was strictly limited by availability of calculation and simulation techniques. It led to necessary production of number of prototypes showing the proper way of construction. The production of extra prototypes generates additional costs which may be reduced using virtual prototyping. The virtual prototyping used in this approach includes analytical design with subsequent verification using electromagnetic FEA (finite element analyses) together with thermal analyses. The proposed design methodology is demonstrated on the HV filter with the following technical requirements (see Tab. I).

TABLE I. REQUIRED PARAMETERS OF DESIGNED FILTER

| | |
|---|---|
| Inductance | $L$=6 [mH] |
| Rated current | $I$=8 [A] (AC, 50/60Hz, sinus wave) |
| Current density | $J$<3 [A/mm$^2$] |
| Ambient temperature | $\vartheta_a$=+40 [°C] |
| Self-frequency range | $f_{crit}$=80÷140 [kHz] |

The first the main dimensions (inner and outer diameter, length of the winding and number of turns) may be calculated using simple analytical equations (1), (2). The number of turns may be found according to expected current density $J$ using:

$$N = 167.2 \sqrt[5]{\frac{J\pi L^2}{4I}} \tag{1}$$

The inner diameter $d$ (diameter of coiling thorn) of the cylindrical coil with several layers is given by the formula:

$$d = \sqrt[5]{\frac{16J^2LI^2}{\pi^2}} \tag{2}$$

The other sizes (see Fig. 3) of the coil are expressed as a function of inner diameter $d$. The outer diameter $D_e$=1.855$d$, central radius $r$=0.714$d$, high of the coil $l$=0.475$d$ and its width $s$=0.428$d$. The model makes the optimization very quick and easy. The goal is to find the balance between minimum sizes (mass) and maximum inductance.

While the analytical approach is very general, fast, transparent and informative its ability to consider the complex geometry is very limited. This may cause unexpected and inestimable error in obtained results. It is therefore necessary to verify given geometry by using some other method. The FEA is suitable for this purpose (Fig. 4).

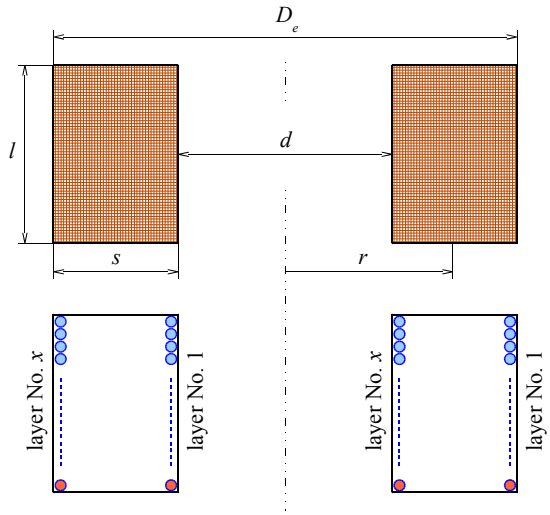


Figure 3. Basic sizes and coil dimensions.

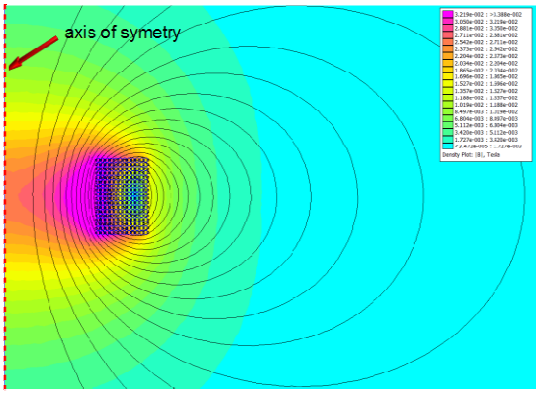


Figure 4. FE model of designed filter.

The coil's inductance can be derived from magnetic energy stored in all electromagnetic regions – winding, air surrounding the winding:

$$W_m = \frac{1}{2}LI^2 \tag{3}$$

As the axisymmetric model used the results are valid only for solenoidal coil, but it is easy to recalculate it even for square coil. The rectangular shaped coil has the same inductance as the cylindrical one with the same area of core and same winding window sizes. The comparison between them shows Tab. II.

TABLE II. CYLINDRICAL AND SQUARE COIL FORM

| **Parameter** | SHAPE OF COIL FORMER | | |
|---|---|---|---|
| | ***cylindrical*** | ***square*** | ***note*** |
| Hollow area | $S_O = \frac{\pi d^2}{4}$ | $S_\square = a^2$ | $d$ … diameter<br>$a$ … rectangle width |
| Condition | $S_O = S_\square \Rightarrow a = \frac{d}{2}\sqrt{\pi}$ | | |
| Circumference | $O_O = \pi d$ | $O_\square = 4a$ | |
| Ratio | $\frac{O_\square}{O_O} = \frac{4a}{\pi d} = \frac{2d\sqrt{\pi}}{\pi d} = \frac{2}{\sqrt{\pi}}$ | | material requirements |

The resulting filter is made from copper wire with 1.9 mm of diameter, total number of turns is divided into 12 layers each coiled from 18 turns. Nominal current 8 A (50 Hz) generates power loss of 72.8 W. All important parameters are summarized in Tab. III.

TABLE III. CONSTRUCTION PARAMETERS OF DESIGNED FILTER

| | |
|---|---|
| Wire diameter | 1.9 [mm] |
| Frequency | 50 [Hz] |
| Rated current | 8 [A] |
| Power losses | 72.8 [W] |
| Total number of turns | 216 [-] |
| Number of turns per layer | 18 [-] |
| Number of layers | 12 [-] |
| *d* \| *s* \| *l* (Fig. 3) | 82 \| 24 \|36 [mm] |
| Mass | 2.5 [kg] |

## III. THERMAL ANALYSIS

The filer requires self-cooling system IC410 (surface cooled by natural convection and radiation) with no external fan to make the measuring system robust, reliable and low-cost. The heat is transferred from the wire through the surface insulation varnish by heat conduction to the coil frame from where it goes directly to the coolant (air) by convection [16, 17]. The outer surface is cooled also by heat convection. The heat transfer coefficient for the outer surface and estimated surface temperature rice $\vartheta$ is as follows:

$$\alpha = 11.3 + 0.08\vartheta \left[\frac{W}{m^2K}\right] \tag{4}$$

For the inner surface the similar formula is used (heat radiation neglected):

$$\alpha = 6.5 + 0.05\vartheta \left[\frac{W}{m^2K}\right], \text{for } \vartheta \in \langle 0|100\rangle\ ^oC \tag{5}$$

The insulating system uses temperature thermal class H (180 °C) with no temperature sensor installed. For the further evaluation the temperature may be determined by DC test (four-terminal sensing method). The simulation (6)-(8) was performed using MATLAB® SW with focusing on heat transfer and system cooling. It is valid for a coil turns located in the middle of each winding layer. The turns close to the coil side (close to coil frame) has a lower temperature. Moreover the heat transfer in the simulation is considered as 2D (not a 3D) vector which means the worst case investigated (see Fig. 5). The thermal conductivity of coil form slightly increases the inner surface temperature with the respect of outer surface temperature. The power losses of winding layer *i* are:

$$\Delta P_i = R_i I^2 [W] \tag{6}$$

The area of cylinder's surface related to certain winding layer *i* can be calculated as:

$$S_i = \pi d_i l [K] \tag{7}$$

The temperature difference of winding layer *i* is as follows:

$$\Delta\vartheta_i = \frac{\Delta P_i}{\alpha S_i}[K] \tag{8}$$

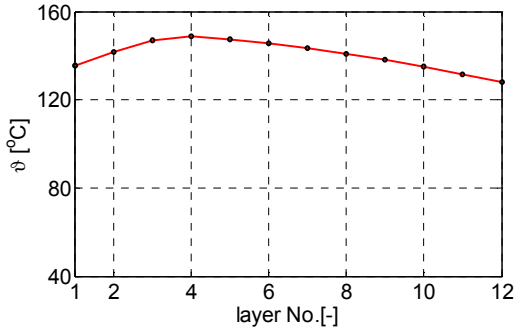


Figure 5. Temperature distribution in the winding

As seen in Fig. 5. the resulting coil has 12 layers of turns. Maximal temperature reaches 149 °C whereas the inner and outer surface temperature are colder (136/128 °C). Ambient temperature is assumed as constant of 40 °C.

## IV. WINDING PARASITIC CAPACITY

The electric field between coils turns has strong impact on parasitic capacity of the coil (see Fig. 6) acting contrary to the inductance and must be reduced as much as possible. On the other hand the capacity is main parameter tuning the self-resonance frequency.

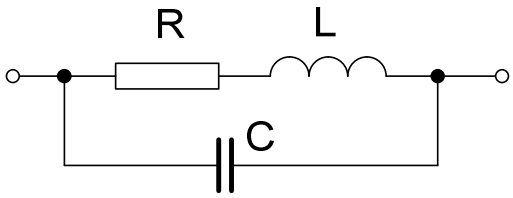


Figure 6. Equivalent circuit of a coil.

It could be set properly by using a special construction (transposed) of the winding (Fig. 7). The transposition makes all neighboring wires decussated and increase their mutual distance.

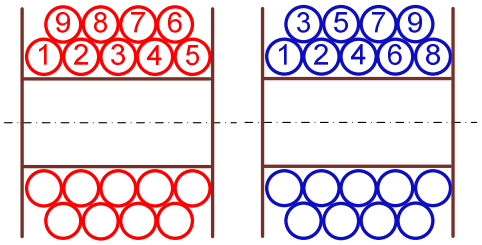


Figure 7. (a) no transposition, (b) transposition - low parasitic capacity.

Another possibility is to divide the winding into several sections according to Fig. 8 and connect them in series. The reduction of parasitic capacity is not as significant as the previous solution exhibits but is retable.

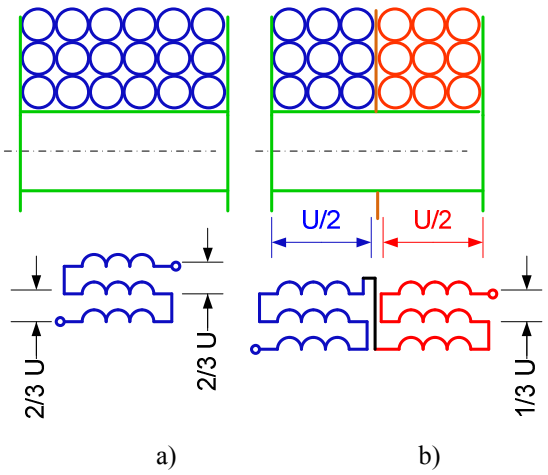


Figure 8. (a) coil with only one section, (b) two sections used

## V. EXPERIMENTS

To make the measurement more accurate the four-terminal sensing method (Kelvin resistance measurement) was used for determination of net resistance (see Fig. 9). Resulting coil inductance was measured using LCR meter.

As seen from Fig. 10 and Fig. 11 all temperatures slightly rises with the loading time (loading current constant) whereas the maximal value of the temperature lies safely under the limit of insulation class of the winding. The red line with cross markers represents the calculated temperature inside the winding (hot spot), the black one with "+" markers is the measured temperature (from winding resistance) and the blue curve with circle markers stands for the temperature measured on the outer surface with thermometer.

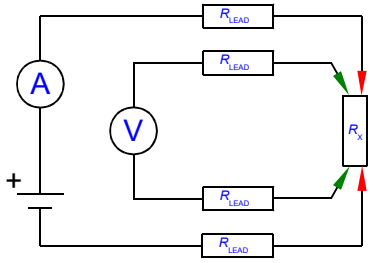


Figure 9. Four-terminal sensing measurement method.

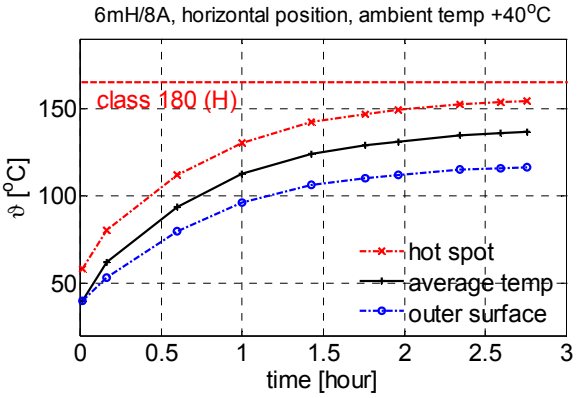


Figure 10. The temperature during the loading test.

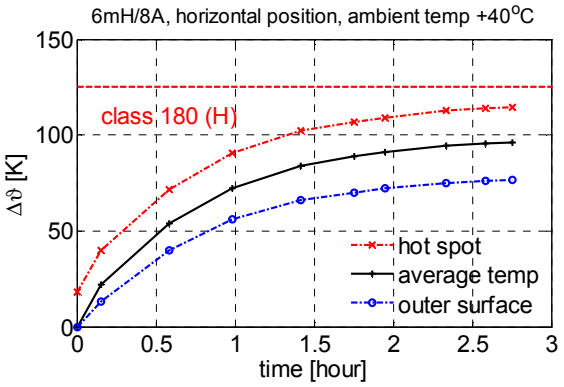


Figure 11. The temperature rise during the loading test.

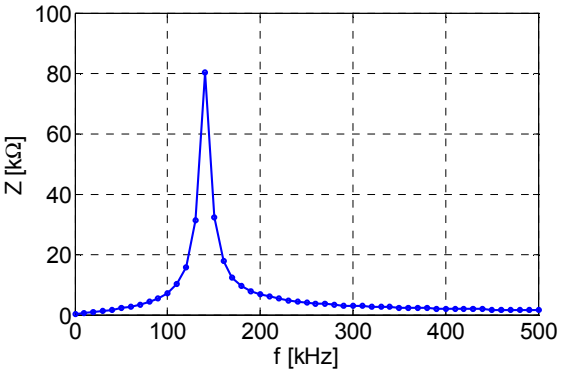


Figure 12. Net impedance as depend on frequency.

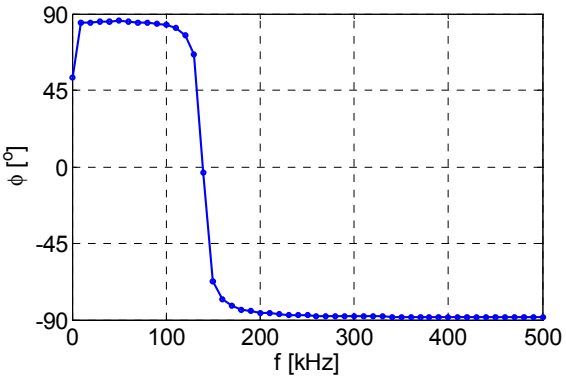


Figure 13. Phase shift between current and voltage (frequency dependent).

The resonance frequency was measured with LCR meter KEYSIGHT®, type E4980A. The net impedance (see Fig. 12) and phase shift (see Fig. 13) between voltage and current were measured for frequency band 20 Hz÷500 kHz (frequency step 10 kHz). From measurement it is clear that the self-resonant frequency ($f_{crit}$) fulfills the requirement from Tab. I.

## VI. CONCLUSION

In light of shape optimization the experimental results indicate relatively sufficient accuracy of proposed design method.

Proposed analytical approach quickly calculates fundamental dimensions together with initial overview of coil's construction lay-out. Introduced thermal model proves ability to predict the temperature

anywhere inside the winding. It can be adopted for any similar geometry and used for any electrical device.

The self-resonant frequency is significantly influenced by parasitic capacity of the winding. It could be balanced by using a special construction of the winding (Fig. 7). Another possible way is to divide the winding into several sections and connect them in series.

## ACKNOWLEDGMENT

This research has been supported by the European Regional Development Fund and the Ministry of Education, Youth and Sports of the Czech Republic under the Regional Innovation Centre for Electrical Engineering (RICE), project no. CZ.1.05/2.1.00/03.0094, TAČR project no. TA02000103 CIDAM and funding program SGS-2012-071.

## REFERENCES

[1] Greg C. Stone, Edward A. Boulter, Ian; "Electrical Insulation for Rotating Machines: Design, Evaluation, Aging, Testing, and Repair", IEEE Press Editorial Board, ISBN 0-471-44506-1, 23 AUG 2004

[2] Shirasaka, Y.; Murase, H.; Okabe, S.; Okubo, H., "Cross-sectional comparison of insulation degradation mechanisms and lifetime evaluation of power transmission equipment," Dielectrics and Electrical Insulation, IEEE Transactions on , vol.16, no.2, pp.560,573, April 2009 doi: 10.1109/TDEI.2009.4815192

[3] Goudie, J.L.; Owen, M.J.; Orbeck, T., "A review of possible degradation mechanisms of silicone elastomers in high voltage insulation applications," Electrical Insulation and Dielectric Phenomena, 1998. Annual Report. Conference on , vol.1, no., pp.120,127 vol. 1, 25-28 Oct 1998, doi: 10.1109/CEIDP.1998.733878

[4] Florkowska, B.; Florkowski, M.; Zydron, P., "The Role of Harmonic Components on Partial Discharge Mechanism and Degradation Processes in Epoxy Resin Insulation," Solid Dielectrics, 2007. ICSD '07. IEEE International Conference on , vol., no., pp.560,563, 8-13 July 2007 doi: 10.1109/ICSD.2007.4290875

[5] J. S. Johnson and M. Warren, "Detection of slot discharges in high-voltage stator windings during operatio," Trans. Am. Inst. Electr. Eng., vol. 70, no. 2, pp. 1998–2000, 1951.

[6] Stone, G.C., "A perspective on online partial discharge monitoring for assessment of the condition of rotating machine stator winding insulation," Electrical Insulation Magazine, IEEE, vol.28, no.5, pp.8,13, September-October 2012

[7] Hudon, C.; Belec, M.; , "Partial discharge signal interpretation for generator diagnostics," Dielectrics and Electrical Insulation, IEEE Transactions on , vol.12, no.2, pp. 297- 319, April 2005 doi: 10.1109/TDEI.2005.1430399

[8] Suwarno; Mizutani, T.; , "Diagnosis of insulation conditions : Interpretation of partial discharges from φ-q-n pattern, pulse-sequence and pulse waveform," Condition Monitoring and Diagnosis, 2008. CMD 2008. International Conference on , vol., no., pp.60-63, 21-24 April 2008 doi: 10.1109/CMD.2008.4580230

[9] Emery, F.T.; "Reduction techniques of partial discharge, dissipation factor, and external corona for high voltage stator windings," Electrical Insulation Conference, 2009. EIC 2009. IEEE , vol., no., pp.315-327, May 31 2009-June 3 2009 doi: 10.1109/EIC.2009.5166364

[10] Mráz, P., Kindl, V., Hruška, K. "Influence of low-conductive coating on insulation system of rotary electric machine", 2012, Journal of Electrical Engineering, 63 (3), pp. 180-185.

[11] Miao Peiqing; Li Xiuwei; Hu Yue; Sheng Gehao; Jiang Xiuchen, "Multi-source separation method for partial discharge detection in substations," Power Engineering and Automation Conference (PEAM), 2012 IEEE , vol., no., pp.1,5, 18-20 Sept. 2012
doi: 10.1109/PEAM.2012.6612543

[12] Liuhuo Wang; Wenjun Ning; Lijun Wang; Hong Lu□; Haijing Wang; Shenli Jia; Ji Wu, "Experimental investigation of partial discharge detection in medium-voltage switchgear based on Ultra-High-Frequency sensor," Electric Power Equipment - Switching Technology (ICEPE-ST), 2013 2nd International Conference on , vol., no., pp.1,4, 20-23 Oct. 2013
doi: 10.1109/ICEPE-ST.2013.6804295

[13] Kreuger, F.H., "Partial discharge detection in high-voltage equipment", London: Butterworths. ISBN 0408020636.

[14] Weber, H. J., "Partial Discharge Measuring Techniques", Tettex-Information 21, 1984

[15] Osvath, P.; Zaengl, W.; "Weber, H. J. Measurement of Partial Discharge – Problems and how they can be solved with a flexible measuring system", Tettex-Information 23,1985

[16] Kanuch, J.; Ferkova, Z., "Simulation and measurement of two-phases synchronous motor with permanent magnets," Maszyny elektryczne : Zeszyty problemove. Vol. 102, no. 2 (2014) ), p. 71-75. - ISSN 0239-3646

[17] Rafajdus, P.; Dubravka, P.; Peniak, A.; "Design procedure of Switch reluctance Motor used for Electric Car Drive," International Symposium on Power Electronic, Electrical Drives, Automation and Motion, 2014. SPEEDAM 2014, pp. 112-117, Jun 18-20, 2014.